DOI: 10.13009/EUCASS2017-275

Carrier deck launching of adapted land-based airplanes

HERNANDO, José-Luis and MARTINEZ-VAL, Rodrigo
Department of Aircraft and Spacecraft
School of Aerospace Engineering
Universidad Politécnica de Madrid
28040Madrid, Spain
joseluis.hernando@upm.es; rodrigo.martinezval@upm.es

Abstract
Harrier VTOL is the basic combat airplane for many Navies, but it will soon be retired from service. Three main alternatives appear: to incorporate another, already existing or under development airplane; to design a completely new aircraft; or to modify an existing land-based airplane for carrier suitability. The present paper is part of a study to assess the feasibility of the third option. In former papers the authors have addressed the compatibility of land-based airplanes with aircraft carriers and the details of the carrier approach guidance and recovery; and showed some major modifications required in wing structure and landing gear. The research proposed here studies the airplane performance during the launching manoeuvre, formed by a take-off run on the flat deck followed by a ski-jump.

1. Introduction

Along its 100 years of existence naval aviation has progressed astonishingly, but it is still one of the most demanding environments for airplane operations: extremely short, moving runways; flight in rough air generated by the vessel's superstructure wake and from the sea surface; etc [1-3].
Modern aircraft carriers are classified into three categories: vessels designed to operate only with thrust vectoring airplanes; ships designed for short take-off and arrested recovery (STOBAR); and carriers equipped with catapults and arresting devices (CATOBAR). This last category requires enormous vessels and, almost always, nuclear propulsion, which is beyond most countries' capabilities [4-6].
Airplanes operating from aircraft carriers perform in two different ways: conventional airplanes that roll on the deck for take-off and landing, although commonly helped by launching and arresting equipment; and vertical/short take-off and landing (V/STOL) aircraft, capable of using its thrust vectoring control (TVC) to become airborne and be recovered vertically or after a extremely short landing run [7]. Therefore, the retirement of VTOL Harriers, announced some years ago in UK and USA, will imply a formidable challenge for many Navies to hold their combat capacity. For Navies with vessel size and equipment other than CATOBAR, three alternative solutions appear: to buy an existing naval airplane, able to takeoff from extremely short runways and being recovered with arresting devices; to design a completely new airplane; and to modify an existing land-based aircraft. The last, solution, if possible, presents very interesting advantages in terms of time and money required.
In former papers the authors have addressed the following items [4, 5, 8]: on the one hand, how to assess the compatibility of land-based airplanes with aircraft carriers; in particular the general characteristics of medium-size carriers and their equipment, in relation to the launching and recovery manoeuvres of airplanes; and on the other hand, the flight dynamics of the carrier approach guidance and recovery stages.
The research described here focusses on the launching manoeuvre, constituted by a take-off run on the flat deck without catapult followed by a ski-jump-assisted lift-off.

DOI: 10.13009/EUCASS2017-275

2. Catapulting or ski-jumping

Adapting land-based airplanes to operate from a carrier deck is a very complex task. At present, only two alternatives can be envisaged: to modify the airplane's structure and equipment to be catapulted; or to use the help provided by a ski-jump further than its own propulsion power. In any of both cases the airplane must be able to get enough lift at the time of leaving the carrier deck; i.e. it will need a suitable combination of speed and angle of attack to counterbalance the relatively high wing loading, although the manoeuvre will also be helped by the wind-on-deck (20 to 25 knots; i.e. 10.3 to 12.9 m/s) generated by the natural wind plus the carrier navigation.
The first solution is out of question for most Navies that have no CATOBAR vessels, although it may be accomplished if the land-based airplane has been designed taking into account this future modifications; as might have been the case for the Dassault Rafale. In the past, the imagination of engineers has generated quite uncommon solutions, aimed at either modifying the attitude of the whole aircraft during take-off, or changing the wing incidence with respect to the fuselage; two such solutions are depicted in Figure 1. The objective in these cases is to allow an adequate angle of attack at the end of the take-off run, compatible with the vertical weight-lift balance. A variant of the nose-up pulled attitude shown is to modify the nose landing gear to allow double extension of the shock absorber up to say 1m (40 inches) as done with British F-4K Phantom. This first solution will not be analysed in the present paper.

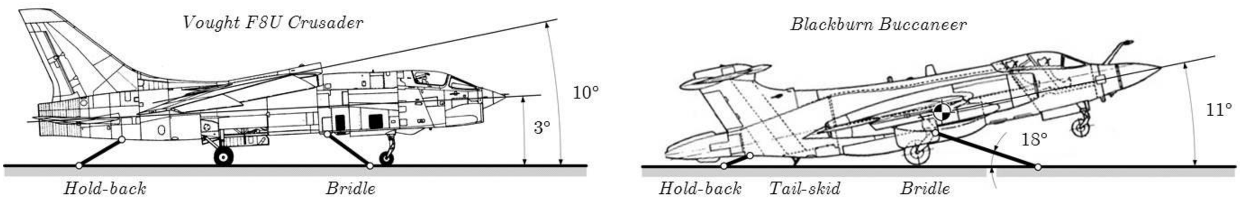

Figure 1. Catapulting with a pivoting variable-incidence wing (left), or with a nose-up rolling attitude (right). Not the same scale.

Ski-jumping is the other alternative [9-11], and is the one that will be described here in some detail. It consists in curving the last part of the deck, as a prolongation of the ship's bow, to impulse the rolling airplane in a climbing trajectory. Commonly, the airplane leaves the deck with less lift than weight and this produces a semi-ballistic path, as shown in Figure 2. Since the airplane continues accelerating along this path, the launching procedure must include enough vertical margin as to avoiding ditching in the ocean. Actually, a minimum clearance is defined, h in Fig. 2, and the airplane increases speed and height from the fly-away point, to match the final airworthy trajectory.

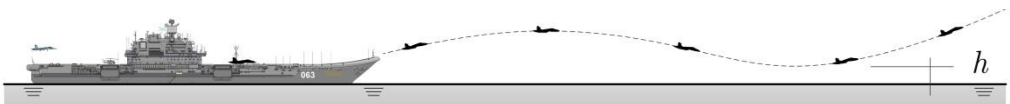

Figure 2. Russian Admiral Kuznetsov, showing ski-jump flying trajectory schematics

Ski-jump is the solution adopted by many Navies, not only with V/STOL airplanes, like AV-8B Harrier II in Spanish Juan Carlos I or Italian Cavour, but also with conventional airplanes, like the Russian Admiral Kutnetsov with Su-33 and Mig-29K, Chinese PLAN Lianoning, with J-15 (a local variant of Su-33), or India's Vikramaditya, with Mig-29K too. This is also the solution adopted for British Queen Elizabeth class new carriers, which will incorporate F-35B Lightning II, one of the versions of American Joint Strike Fighter.
Given the nature and complexity of the airplane-carrier integration process, it is highly convenient to build test facilities where all parameters and modifications can be checked during the early stages of the process, before attempting the actual on-carrier operation. Some of them were very active in the past, but have been closed for budgetary and obsolescence, as those presented in Figure 3.

DOI: 10.13009/EUCASS2017-275

Figure 3. (Left): AV-8A trials at RAE Bedford (1977), with a 6-20º adjustable ramp. (Right), Sea Harrier FRS.1 exhibition at Farnborough Festival, 1978.

At present there are only four main facilities, categorised SBTF (for Shore Based Test Facilities):

- NAS Patuxent River, Maryland, USA.
- Ground Test Aviation Training Complex (NITKA), located in a former Soviet Naval Aviation base at Crimea (Ukraine), operated by the Russian Navy.
- Naval Air Station Hansa, at Goa, India.
- Naval Air Training Facility (NATF) at Huangcun, a military airfield in Liaoning province, used for crew training operations.

Further to these major test fields, the University of Science and Technology at Wuhan, China, has a singular building, with a full-scale carrier deck built on the roof, including a ski-jump.

3. Ski-jumping manoeuvre analysis

This chapter describes the ski-jumping manoeuvre for a conventional airplane without thrust vectoring capacity. The analysis is carried out in three steps: firstly, the rolling on the deck, flat part and up-curved end; secondly, the semi-ballistic flight just after leaving the deck; and last, wind-on-deck effects.

3.1 Rolling phase

The forces acting on the airplane while rolling on the deck lead to the equations below [12, 13]. In this situation wind axes coincide with local horizon axes (see Figure 4).

$$
\begin{aligned}
&T\cos\left(\theta_0+\varepsilon\right)-D-F_f=\frac{W}{g}\frac{dv}{dt}\\
&L+T\sin\left(\theta_0+\varepsilon\right)+N-W=0
\end{aligned}
\qquad (1)
$$

Where θ_0 is the angle between the aircraft longitudinal reference axis and the local horizon, ε is the misalignment between thrust (T) and airplane reference axis, W is weight, L lift, D drag, N vertical ground reaction and F_f the friction ground reaction. These equations can be integrated through the two phases: flat roll and curved ski-jump (with end angle of θ_f as shown in Figure 4). This integration provides the following approximate results which are adequate for preliminary analysis as this one.

$$
v_I=\left(\frac{2}{1.02}g\frac{\overline{T}}{W}L_{Deck}\right)^{0.5} \qquad (2)
$$

$$
v_{II}=\left\{v_I^2+\frac{2}{1.02}g\left[s_{SJ}\frac{\overline{T}}{W}-\overline{R}\left(1-\cos\theta_f\right)\right]\right\}^{0.5} \qquad (3)
$$

DOI: 10.13009/EUCASS2017-275

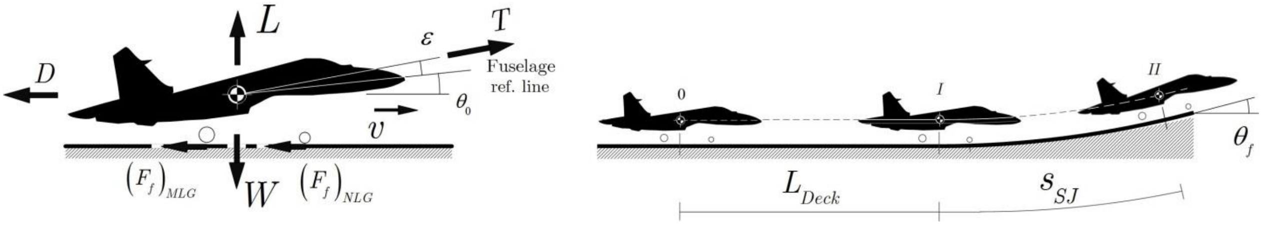

Figure 4. Main forces and angles (left), and the two stages considered on an aircraft rolling on a carrier deck with ski-jump at the end.

The integration has been simplified [14] by taking $\overline{T}$ as an average, constant thrust, and by considering the ski-jump as a constant radius, $\overline{R}$, shape with $s_{SJ} = \overline{R}\theta_f$

3.2 Semi-parabolic phase

Once the airplane loses contact with the carrier deck, the equations of motion, in local horizon axes, are [8, 12, 13].

$$
\begin{aligned}
&T\cos(\theta+\varepsilon) - L\sin(\theta-\alpha) - D\cos(\theta-\alpha) = \frac{W}{g}\ddot{x}_G \\
&L\cos(\theta-\alpha) - D\sin(\theta-\alpha) + T\sin(\theta+\varepsilon) - W = \frac{W}{g}\ddot{z}_G \qquad (4) \\
&M_G = I_y\ddot{\theta}
\end{aligned}
$$

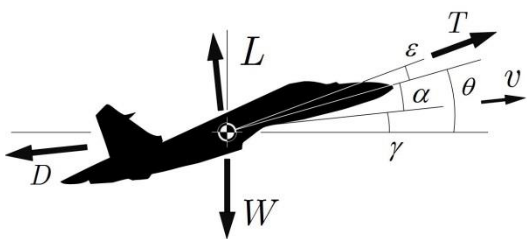

Figure 5. Forces and angles on a flying aircraft, reduced to center of mass

By definition, $\theta = \alpha + \gamma$, $D = qSC_D(\alpha)$, $L = qSC_L(\alpha)$, $M_G = qS\bar{c}\,C_{M_G}$. The initial conditions of this semi-parabolic flight, at t=0, are

$$\dot{x}_G(0) = v_{II}\cos\theta_0;\ \dot{y}_G(0) = v_{II}\sin\theta_0;\ q(0) = \frac{1}{2}\rho v_{II}^2;\ \frac{d\theta}{dt}(0) = v_{II}/\overline{R};\ \alpha(0) = \theta_0;\ \theta(0) = \theta_0 + \theta_f,$$

$$x_G(0) = 0;\ \dot{y}_G(0) = 0;$$

To integrate the former equations, values for $T/W,\ W/S,\ I_y,\ S,\ \bar{c}$ (mean aerodynamic chord) are needed. Common aerodynamic coefficients will be used, $C_L,\ C_D,\ C_{M_G}$, with the last coefficient depending on the airplane configuration; i.e. conventional, tailless, canard, etc, leading to

$$C_L = C_{L0} + C_{L\alpha}\alpha + C_{L\delta}\delta$$

$$C_D = C_{D0} + kC_L^2$$

The equations have been integrated by means of a 4th order Runge-Kutta method.

DOI: 10.13009/EUCASS2017-275

4.3 Wind-on-deck effects

Let's consider a certain u_w wing component which is assumed to be perfectly aligned with the carrier deck take-off runway. This wind is solely generated by the vessel's movement. From Figure 6, it can be deduced that

$$\Delta\alpha = \theta_f - \arctan\left(\frac{\sin\theta_f}{\cos\theta_f + \frac{u_w}{v_{II}}}\right) \tag{5}$$

$$v_T = v_{II}\left[1 + \left(\frac{u_w}{v_{II}}\right)^2 + 2\frac{u_w}{v_{II}}\cos\theta_f\right]^{0.5}$$

The initial conditions are modified by the wind-on-deck as

$$q_{WOD}(0) = \frac{1}{2}\rho v_T^2,\ \frac{d\theta}{dt}(0) = v_{II} / \overline{R},\ \alpha_{WOD}(0) = \theta_0 + \Delta\alpha,\ \theta(0) = \theta_0 + \theta_f.$$

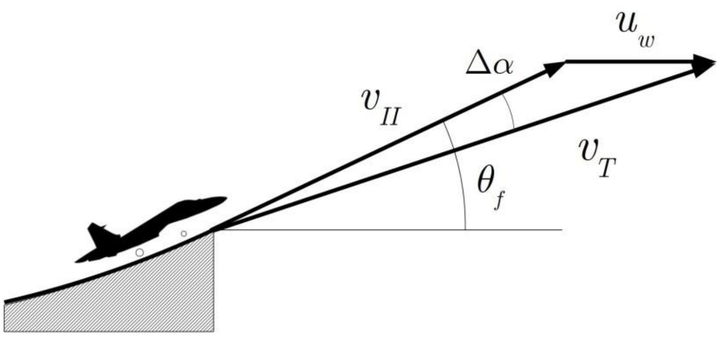

Figure 6. Kinematics with wind on deck

4. Design case

As it is obvious, this process is very complex, with too many variables intervening, some from the ship, and some from the aircraft. To clarify the analysis, the present paper considers the case of Eurofighter Typhoon (EFA, [15]) taking-off from a Spanish LHD Juan Carlos I (Figure 7). The objective is to assess the feasibility of such airplane-carrier combination, with the least modifications for both and without severely compromising the tactical performances of the combat airplane. The key parameters are

$$L_{deck} = 175\text{ m};\ \theta_f = 12^o;\ \overline{R} = 165\text{ m};\ s_{SJ} = \overline{R}\theta_f = 34.56\text{ m}$$

$$T/W \equiv T_{\max}/MTOW = 0.77;\ W/S = 23500\times 9.81/51.2 = 4502.64\text{ N/m}^2;$$

$$v_{II} = 55.09\text{ ms}^{-1};\ u_w = 25\text{ kn} = 12.85\text{ m/s} \quad \Rightarrow \Delta\alpha = 2.26^o;\ v_T = 67.71\text{ ms}^{-1}$$

$$q_{WOD}(0) = \frac{1}{2}1.225\times 67.71^2 = 2807.89\text{ Nm}^{-2},\ \frac{d\theta}{dt}(0) = 55.09/165 = 0.334\text{ s}^{-1}$$

$$\varepsilon \equiv 0^o;\ \theta_0 \equiv 1^o;\ \alpha_{WOD}(0) = 1 + 2.26 = 3.26^o,\ \theta(0) = 13^o$$

$$I_y = 280592\text{ Nms}^2;\ \overline{c} = 5.69\text{ m};$$

The runway length is taken as the largest possible, L_{deck}, just clearing the stern lift.

DOI: 10.13009/EUCASS2017-275

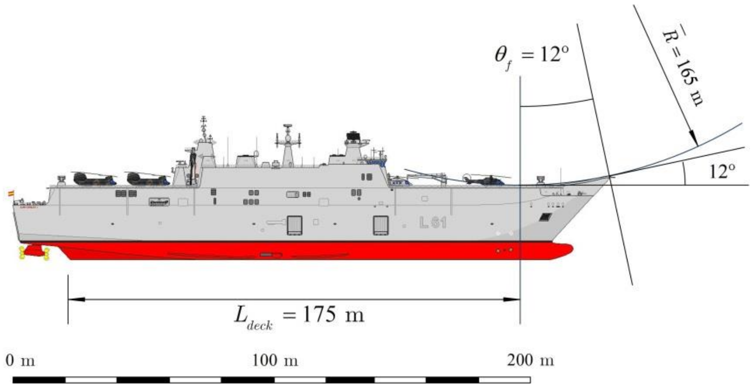

Figure 7. Spanish flagship LHD Juan Carlos I, showing measurements considered

4.1 Estimation of aircraft aerodynamics

The Eurofighter has a swept canard/staggered-delta wing configuration (figure 8). Thus

$$C_L = (C_L)_w + (C_L)_c \frac{S_c}{S}$$
$$C_D = (C_D)_{wb} + (C_D)_c \frac{S_c}{S} \quad (6)$$

where $\alpha_c = \alpha + \delta_c$, $\alpha_w \approx \alpha$, $q_c \approx q$, $C_{Lwb} \approx C_{Lw}$, are assumed. The canard deflection angle, δ_c, is positive upwards.

The aerodynamic characteristics of the wing can be estimated [16-20] by considering inboard and outboard flaperons deflected the same angle, δ (positive downward):

$$(C_L)_w\big|_{\delta=0} = 2.66\sin\alpha\cos^2\alpha + 2.867\cos\alpha\sin^2\alpha$$
$$(C_L)_w\big|_{\delta=10^\circ} = 2.66\sin(\alpha+3.98^\circ)\cos^2(\alpha+3.98^\circ) + 2.867\cos(\alpha+3.98^\circ)\sin^2(\alpha+3.98^\circ) \quad (7)$$
$$(C_L)_w\big|_{\delta=20^\circ} = 2.66\sin(\alpha+6.71^\circ)\cos^2(\alpha+6.71^\circ) + 2.867\cos(\alpha+6.71^\circ)\sin^2(\alpha+6.71^\circ)$$

$$(C_D)_{wb}\big|_{\delta=0} = 0.02 + 2.66\sin^2\alpha\cos\alpha + 2.867\sin^3\alpha$$
$$(C_D)_{wb}\big|_{\delta=10^\circ} = 0.030917 + 2.66\sin^2(\alpha+3.98^\circ)\cos(\alpha+3.98^\circ) + 2.867\sin^3(\alpha+3.98^\circ) \quad (8)$$
$$(C_D)_{wb}\big|_{\delta=20^\circ} = 0.041835 + 2.66\sin^2(\alpha+6.71^\circ)\cos(\alpha+6.71^\circ) + 2.867\sin^3(\alpha+6.71^\circ)$$

Regarding the aerodynamic drag, and to be on the conservative side of the estimation, the airplane is assumed to be airworthy with its maximum take-off weight and all 13 external stations occupied by missiles, bombs, fuel tanks, etc. The canard contribution can be estimated as:

$$(C_L)_c \frac{S_c}{S} = 2\pi \times 8.57\times10^{-3}\frac{4.54}{51.2}\alpha_c(^\circ) = 4.77\times10^{-3}\alpha_c(^\circ) \square (C_L)_w \quad (9)$$

$$(C_{D0})_c \square (C_{D0})_{wb}\frac{S_c}{S} = (C_{D0})_{wb}\frac{4.54}{51.2} \quad (10)$$

DOI: 10.13009/EUCASS2017-275

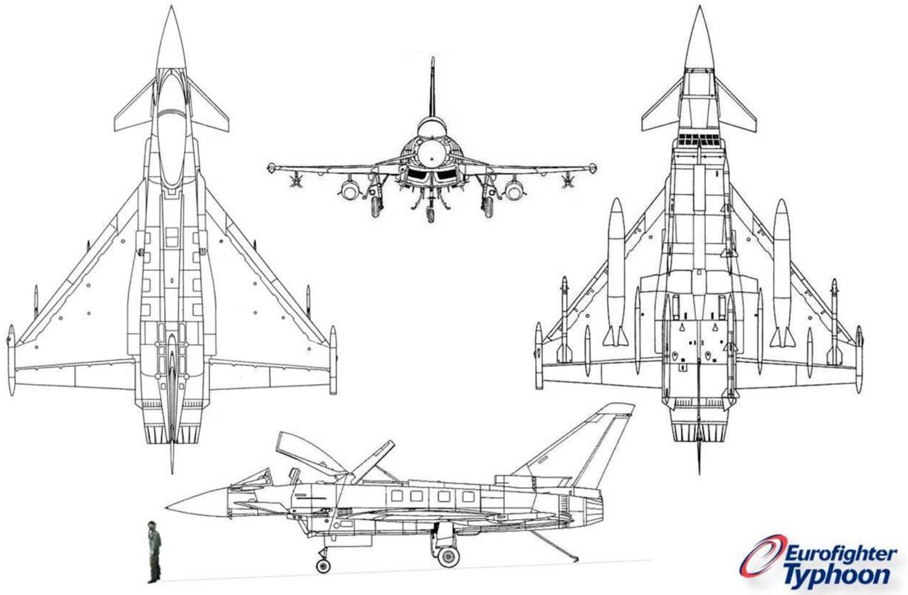

Figure 8. Eurofighter Typhoon, four views.

The pitching moment equation for a canard airplane is (with forces shown in Figure 9):

$$
\begin{aligned}
&M_G = \left(M_{ac}\right)_{wb} - \left[L_w \cos\left(\theta-\gamma\right) + D_w \sin\left(\theta-\gamma\right)\right] d_{ac} + \left(M_G\right)_c \\
&\left(M_G\right)_c = \left[L_c \cos\left(\theta-\gamma\right) - D_c \sin\left(\theta-\gamma\right)\right] d_c + \left[L_c \sin\left(\theta-\gamma\right) + D_c \cos\left(\theta-\gamma\right)\right] z_c + \left(M_{ac_c}\right)_c \\
&C_{M_G} = \left(C_{M_{ac}}\right)_{wb} - \left[\left(C_L\right)_w \cos\alpha + \left(C_D\right)_{wb} \sin\alpha\right] \frac{d_{ac}}{\bar{c}} + \left(C_{M_G}\right)_c \frac{S_c}{S} \frac{\bar{c}_c}{\bar{c}} \qquad (11) \\
&\left(C_{M_G}\right)_c = \left[\left(C_L\right)_c \cos\alpha - \left(C_D\right)_c \sin\alpha\right] \frac{d_c}{\bar{c}_c} + \left[\left(C_L\right)_c \sin\alpha + \left(C_D\right)_c \cos\alpha\right] \frac{z_c}{\bar{c}_c} + \left(C_{M_{ac}}\right)_c \\
&\qquad \approx \left(C_L\right)_c \cos\alpha \frac{d_c}{\bar{c}_c} + \left(C_{M_{ac}}\right)_c
\end{aligned}
$$

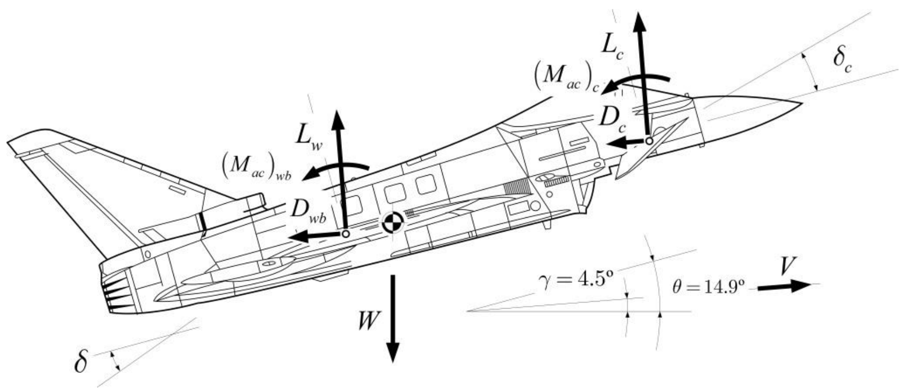

Figure 9. Eurofighter Typhoon attitude at fly-away point, showing forces, moments and angles.

DOI: 10.13009/EUCASS2017-275

If a common flaperon deflection of $\delta = 20^{\text{o}}$ is considered, then

$$\begin{aligned}
C_L\big|_{\delta=20^{\text{o}}} &= \left(C_L\right)_w\big|_{\delta=20^{\text{o}}} + 2\pi\times 8.57\times 10^{-3}\,\frac{4.54}{51.2}\,\alpha_c\left(^{\text{o}}\right) \approx \left(C_L\right)_w\big|_{\delta=20^{\text{o}}} \\
C_D\big|_{\delta=20^{\text{o}}} &= \left(C_D\right)_{wb}\big|_{\delta=20^{\text{o}}} + \left(C_{D0}\right)_c = \left(C_D\right)_{wb}\big|_{\delta=20^{\text{o}}} + 4.18\times 10^{-2}\,\frac{4.54}{51.2} \\
C_{M_G}\big|_{\delta=20^{\text{o}}} &= \left(C_{M_{ac}}\right)_{wb}\big|_{\delta=20^{\text{o}}} + \left(C_{M_G}\right)_c \frac{S_c}{S}\frac{\bar{c}_c}{\bar{c}} - \frac{d_{ac}}{\bar{c}}\left[\left(C_L\right)_w\big|_{\delta=20^{\text{o}}}\cos\alpha + \left(C_D\right)_{wb}\big|_{\delta=20^{\text{o}}}\sin\alpha\right]
\end{aligned} \tag{12}$$

It can be noticed that the airplane is stable, since the terms depending upon the angle of attack are all negative.

$$C_{M_G}\big|_{\delta=20^{\text{o}}} = \underbrace{\left(C_{M_{ac}}\right)_{wb}\big|_{\delta=20^{\text{o}}} + \left(C_{M_G}\right)_c \frac{S_c}{S}\frac{\bar{c}_c}{\bar{c}}}_{\left(C_{M_G}\right)_0} - \underbrace{\frac{d_{ac}}{\bar{c}}\left[\left(C_L\right)_w\big|_{\delta=20^{\text{o}}}\cos\alpha + \left(C_D\right)_{wb}\big|_{\delta=20^{\text{o}}}\sin\alpha\right]}_{f(\alpha)} \tag{13}$$

When the aircraft finishes the impulse manoeuvre (*fly-away point)*, it will be flying at an angle of attack α_{fap} such that

$$M_G = I_y\ddot{\theta} = 0 \;\;\Rightarrow\;\; C_{M_G}\big|_{\delta=20^{\text{o}}}\left(\alpha_{fap}\right) = 0 \tag{14}$$

that implies:

$$\left[\left(C_{M_{ac}}\right)_{wb}\big|_{\delta=20^{\text{o}}} + \left(C_{M_G}\right)_c \frac{S_c}{S}\frac{\bar{c}_c}{\bar{c}}\right]\frac{\bar{c}}{d_{ac}} = \left(C_L\right)_w\Big|_{\delta=20^{\text{o}}}^{\alpha_{fap}}\cos\alpha_{fap} + \left(C_D\right)_{wb}\Big|_{\delta=20^{\text{o}}}^{\alpha_{fap}}\sin\alpha_{fap} \tag{15}$$

which, as it can be shown, for $\alpha_{fap} = 10^{\text{o}}$ and $d_{ac}/\bar{c} = 0.1$ leads to

$$\left(C_{M_{ac}}\right)_{wb}\big|_{\delta=20^{\text{o}}} + \left(C_{M_G}\right)_c \frac{S_c}{S}\frac{\bar{c}_c}{\bar{c}} = 0.97017\,\frac{d_{ac}}{\bar{c}} \cong 0.1 \tag{16}$$

$$\begin{aligned}
C_L\big|_{\delta=20^{\text{o}}} &= 2.66\sin\left(\alpha+6.71^{\text{o}}\right)\cos^2\left(\alpha+6.71^{\text{o}}\right) + 2.867\cos\left(\alpha+6.71^{\text{o}}\right)\sin^2\left(\alpha+6.71^{\text{o}}\right) \\
C_D\big|_{\delta=20^{\text{o}}} &= 0.0455 + 2.66\sin^2\left(\alpha+6.71^{\text{o}}\right)\cos\left(\alpha+6.71^{\text{o}}\right) + 2.867\sin^3\left(\alpha+6.71^{\text{o}}\right) \\
C_{M_G}\big|_{\delta=20^{\text{o}}} &= 0.1 - 0.1\left[\left(C_L\right)_w\big|_{\delta=20^{\text{o}}}\cos\alpha + \left(C_D\right)_{wb}\big|_{\delta=20^{\text{o}}}\sin\alpha\right]
\end{aligned} \tag{17}$$

The last equation is equivalent to

$$\begin{aligned}
0.1 &= \left(C_{M_{ac}}\right)_{wb}\big|_{\delta=20^{\text{o}}} + \left[\frac{d_c}{\bar{c}}\left(C_L\right)_c\cos\alpha + \frac{\bar{c}_c}{\bar{c}}\left(C_{M_{ac}}\right)_c\right]\frac{S_c}{S} \\
&= \left(C_{M_{ac}}\right)_{wb}\big|_{\delta=20^{\text{o}}} + 0.2608\alpha_c\left(\text{rad}\right)\times\cos\alpha + 0.0166\left(C_{M_{ac}}\right)_c
\end{aligned}$$

where some assumptions have been done, such as $d_c/\bar{c} = 0.9543;\;\; \bar{c}_c/\bar{c} = 0.1878$. The canard control law is estimated to be

$$\alpha_c\left(\text{rad}\right) = \left[0.2834 - 3.83\left(C_{M_{ac}}\right)_{wb}\big|_{\delta=20^{\text{o}}} - 0.064\left(C_{M_{ac}}\right)_c\right]\sec\alpha$$

DOI: 10.13009/EUCASS2017-275

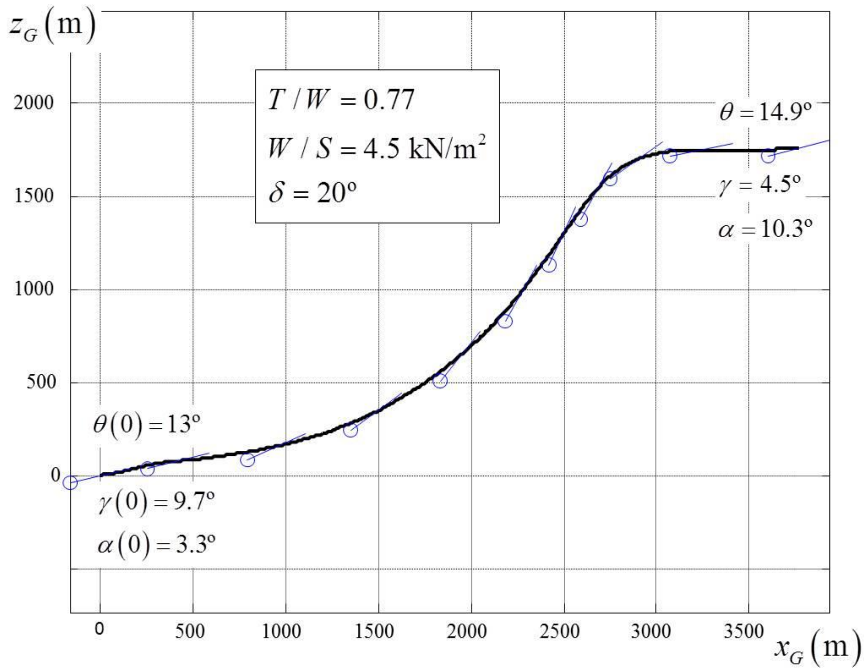

Figure 10. Flight path and airplane attitude for *T/W*=0.77, *W/S*=4.5 kN/m^2 and delta=20º.

As an example of the results, Figure 10 depicts the trajectory of the aircraft after leaving the carrier deck. The path evolves in an uncommon manner, firstly by gaining angle of attack, to increase lift, and later by gaining altitude. After a minute, approximately, the airplane has reached a rather ordinary flight condition.

5. Conclusions

The present paper has been devoted to assess the feasibility of launching an advanced combat airplane from a mid-size carrier, without entering into the complex analysis of how such aircraft would board the vessel, topic that would deserve a specific study.

As an example of critical aircraft/vessel combination Eurofighter Typhoon (EFA) and Juan Carlos I have been used. Needless-to-say, any analysis on the aircraft/vessel compatibility topic is highly specific and cannot be extrapolated to another combination.

In this research a number of aerodynamic features of the aircraft have been estimated, with methods proper of preliminary design and, therefore, the findings presented here have such depth level.

The key finding is that EFA is capable of safely operate from a mid-size carrier without catapult, and the only help of a ski-jump on the ship's bow. The fly-away from the end of the curved deck follows a trajectory compatible with common piloting practice.

Interestingly, the aircraft requires no major modifications for the launching manoeuvre, as opposed to what can be expected from the recovery, this last due to the much higher than normal vertical speed at touchdown in sea approaches.

This preliminary study has been carried out with the original all up weight. This means that the land-based airplane could perform the manoeuvre without being penalized for the requirement of taking-off from a carrier, and would keep all its combat capability.

Additional research is necessary to confirm the preliminary results, to assess the effectiveness of thrust vectoring control, and to optimize piloting control laws and airplane attitude during the initial fly-away phase.

DOI: 10.13009/EUCASS2017-275

Acknowledgments

The authors want to express their gratitude to Dr. Enrique de la Fuente, for his comments and help with the programming of equations.

References

[1] Friedman N, 1983. US aircraft carrier: an illustrated design history. Annapolis, MD, USA, Naval Institute Press.
[2] Lawrence T, 2003. Milestones and developments in US naval carrier aviation. AIAA atmospheric flight mechanics conference, Austin, TX, AIAA paper 2003-5543.
[3] Lawrence T, 2005. Milestones and developments in US naval carrier aviation-Part II. AIAA atmospheric flight mechanics conference, San Francisco, CA, AIAA paper 2005-6120.
[4] Hernando JL and Martinez-Val R, 2012. Carrier suitability of land-based aircraft. Paper 167 28th ICAS Congress, Brisbane, Australia, 23-28 September.
[5] Hernando JL and Martinez-Val R, 2015. Preliminary suitability analysis of carrier approach guidance and recovery of land-based aircraft. Proc IMechE Part G. 230: 906-920.
[6] Polmar N, 2007. Aircraft carriers: a history of carrier aviation and its influence on world events. Potomac Books, Inc. Garden City, NY, USA.
[7] Ikaza D, 2000. Thrust vectoring nozzle for modern military aircraft. In NATO R&T Organization symposium on active control technology for enhanced performance operational capabilities of military aircraft, land vehicles and sea vehicles, Braunschweig (Germany), Paper no. RTO-MP-051, pp.11.1--11.10.
[8] Hernando JL, 2016. Carrier suitability of land-based aircraft (original in Spanish, sic: «Análisis de la embarcabilidad de aviones de combate terrestres»). PhD Thesis. School of Aerospace Engineering. Technical University of Madrid (UPM). https://doi.org/10.20868/UPM.thesis.40985
[9] Turner EW, 1991. Aircraft operations from runways with inclined ramps (ski-jump). Report WRDC-TM-90-337-FIBE. Wright Laboratory. Loads and criteria group, Structures Division. Flight Dynamics Directorate. Air Force Systems Command. Wright-Patterson AFB, Ohio.
[10] Birckelbaw L, 1992. Ski jump takeoff performance predictions for a mixed-flow, remote-lift STOVL aircraft. NASA TM 103866, NASA Ames Research Center.
[11] Fry A, Cook R and Revill N, 2009. CVF ski-jump ramp profile optimisation for F-35B. The Aeronautical Journal. 113:79-85.
[12] Anderson JD, 1999. Aircraft performance and design. McGraw-Hill, Singapore.
[13] Yechout TR, Morris SL, Bossert DE et al, 2014. Introduction to aircraft flight mechanics: performance, static stability, dynamic stability, and classical feedback control, 2nd edition. AIAA, Reston, VA, USA.
[14] Anonymous, 1999. Catapulting and arresting gear forcing functions for aircraft structural design. MIL-HDBK-2066 (AS), Department of Defense Handbook. Naval Air Systems Command, Department of the Navy, Arlington, VA, USA.
[15] Anonymous, 2013. Eurofighter Typhoon Technical Guide, Issue 01-2013. Eurofighter Jagdflugzeug GmbH, Hallbergmoos, Germany.
[16] Polhamus EH, 1966. A concept of the vortex lift of sharp-edge delta wings based on a leading-edge suction analogy. NASA Technical Note D-3767. National Aeronautics and Space Administration, Washington DC, USA.
[17] Polhamus EH, 1968. Application of the leading-edge-suction analogy of vortex-lift to the drag due to lift on sharp-edge delta wings. NASA Technical Note D-4739. National Aeronautics and Space Administration, Washington, DC, USA.
[18] Polhamus EH, 1971. Charts for predicting the subsonic vortex-lift characteristics of arrow, delta, and diamond wings. NASA Technical Note D-6243. National Aeronautics and Space Administration, Washington, DC, USA.
[19] Roskam L and Lan CTE, 1997. Airplane aerodynamics and performance. DAR Corporation, Lawrence, KS, USA.
[20] Nicolai LM and Carichner GE, 2010. Fundamentals of aircraft and airship design. AIAA, Reston, VA, USA.